ISSN 0001-4370, Oceanology, 2009, Vol. 49, No. 3, pp. 299–309. © Pleiades Publishing, Inc., 2009.
Original Russian Text © V.G. Bondur, Yu.V. Grebenyuk, K.D. Sabinin, 2009, published in Okeanologiya, 2009, Vol. 49, No. 3, pp. 325–336.

MARINE PHYSICS

Peculiarities of Internal Tidal Wave Generation near Oahu Island (Hawaii)

V. G. Bondur[a], Yu. V. Grebenyuk[a], and K. D. Sabinin[b]

[a] *"Aerokosmos" Scientific Center for Aerospace Monitoring, Moscow, Russia*
E-mail: vgbondur@aerocosmos.info

[b] *Space Research Institute, Russian Academy of Sciences, ul. Profsoyuznaya 84/32, Moscow, 117997 Russia*

Abstract—The peculiarities of the internal tidal wave generation in Mamala Bay (Oahu Island, Hawaii) have been studied based on an analysis of the measurements of the current and temperature profiles and the CTD data in this region. ITs of local origin, which differ from waves of distant origin (predominant in the bay) by the presence of high-order modes, have been detected by using special methods for processing current velocities obtained with the help of ADP acoustic meters. The data of the profilers have been analyzed by using empirical orthogonal functions. It has been established that waves of local origin radiating from the shelf edge into the ocean are also present in the total IT field.

DOI: 10.1134/S0001437009030011

INTRODUCTION

ITs near Hawaii have been intensely studied, e.g., within the scope of the HOME program [9, 17, 21, 23, 24] and during earlier experiments [16, 25]; nevertheless, many aspects remain unclear because the IT field is extremely complex at the Hawaiian Ridge in general and in Mamala Bay near Oahu Island in particular. This experiment indicated that the IT sources are, as a rule, concentrated at large depths because the Hawaiian Ridge slopes are very steep (see Fig. 1) [17, 21, 23, 24].

The IT generation on the continental slope substantially changes in different areas depending on the bottom inclination and the density stratification, which is responsible for the inclination of the IT energy propagation trajectory (the slope of the characteristic line or beam). The beam inclination depends on the wave frequency, the inertial frequency, and the buoyancy frequency [7] and increases with decreasing buoyancy frequency. When the inclinations of a beam and the bottom coincide, the energy of a barotropic tide is effectively transferred to an internal baroclinic tide, the amplitude of which becomes large in the bottom layers. If the inclinations of a beam and bottom are different, the oscillations insignificantly intensify at the bottom.

An analysis of the Mamala Island bottom topography indicates that a rather abrupt increase in depths with a bottom inclination of ~12° is observed at a small distance from the Sand Island outfall diffuser (Figs. 1c–1e). An IT beam can be effectively reflected from a bottom if it propagates at the same angle, which is reachable at a low buoyancy frequency. For the average stratification density in Mamala Bay, the bottom inclination at the shelf edge is supercritical; therefore, it is considered that an IT is generated here at depths of 500–1000 m, where the semidiurnal tide beams become steeper and coincide with the bottom inclination due to the decreasing stratification [16, 23], rather than above a shelf edge as is usual. The semidiurnal IT radiates precisely from these depths of the critical inclination but only into the open ocean since the inclination of the bottom is higher than that of the beam up the slope.

Nevertheless, considerable ITs are observed at the edge of the Mamala Bay shelf [2–5]. Based on the data on the considerable (up to 50 m) semidiurnal vertical thermocline fluctuations at the shelf edge in Mamala Bay, Hamilton [16] assumed that these fluctuations are related to a loop in the system of quasistationary waves, which originates at the bay center due to convergence of tidal currents that come from both sides of Oahu Island. According to Hamilton, precisely these fluctuations are the source of local generation of ITs, from which these tides are radiated into the open ocean.

The following modeling and field observations [4, 5, 9, 12, 17, 21, 23, 24] indicated that this is not the case and the considerable semidiurnal ITs in the bay are related to distant sources above rapids in the straits on both sides of Oahu Island (Fig. 1a). When these waves arrive at the bay, they form a complex interference field varying not only in space but also in time because of a change in the background conditions. Based on an analysis of the observations at the edge of the Mamala Island shelf, we can nevertheless assume (as was done in [4]) that local generation is also observed here, at least sporadically, under favorable conditions.

Since locally generated ITs are masked by waves coming from straits, it is difficult to extract these tides from the total fluctuations. In the present work, the tides are detected based on the following signs of locally radiated ITs:

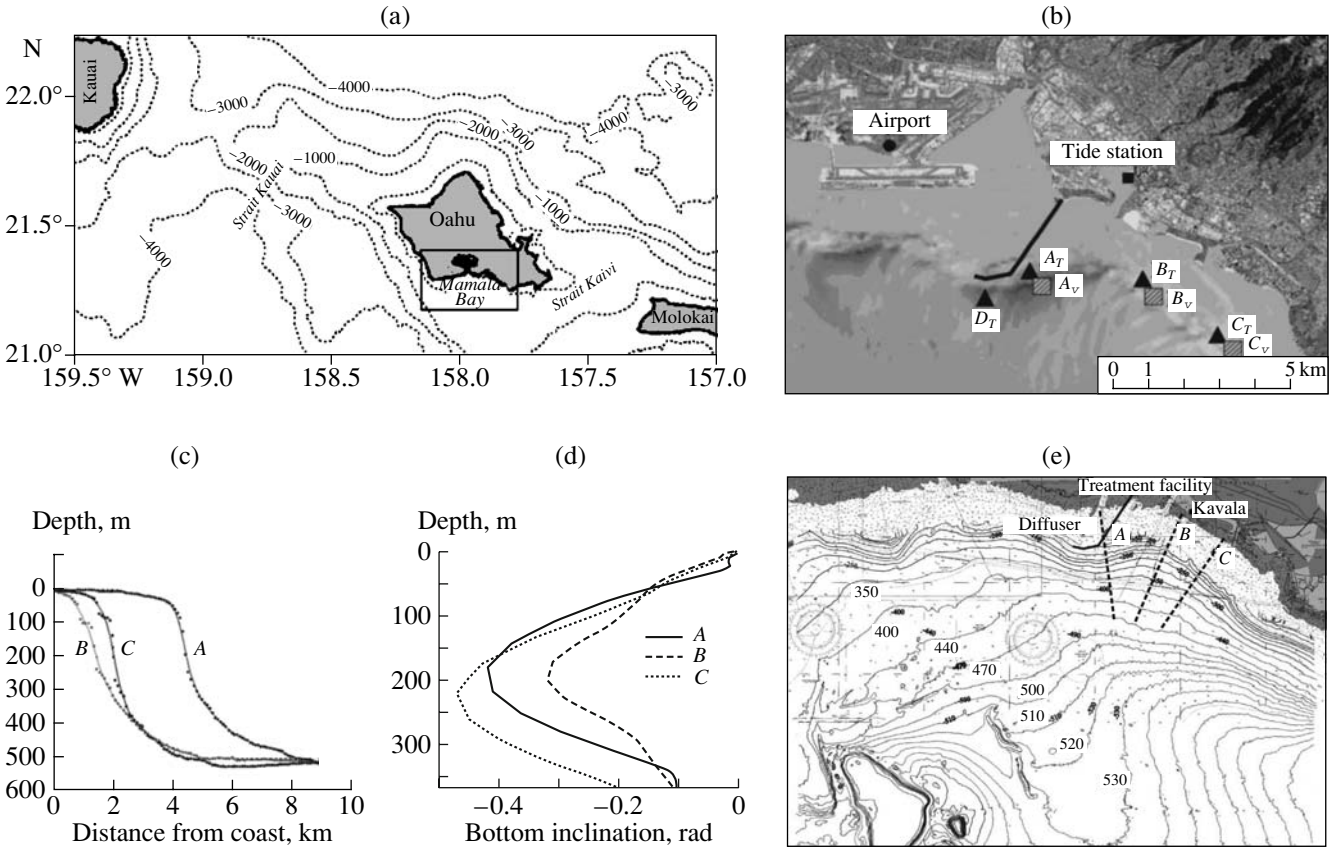

Fig. 1. Oahu Island and Mamala Bay: (a) a geographic and bathymetric map of the water area in the Oahu region; (b) the location of the stationary stations for measuring the temperature and current velocities in the bay; the profiles of (c) the depth and (d) bottom inclination along sections *A*–*C* shown on the map of the bottom topography (e).

(1) The ratio of the minor and major axes of the current hodographs should be close to the ratio of the local inertial frequency ($f = 0.03$ cycle h^{-1}) to the frequency of the semidiurnal M2 IT (0.0805 cycle h^{-1}) equal to 0.38.

(2) The orbits should be elongated along the normal to the isobaths at the shelf edge.

(3) The waves should have a ray structure typical of the IT field in the near zone. In this case, a waveform near a source propagates downward, which corresponds to upward motion of oblique wave energy.

The following factors of local IT generation are less definite but, nevertheless, substantial:

(1) a decrease in the density stratification (buoyancy frequency) in the lower section of the water body above the shelf edge, as a result of which the IT beams become steeper;

(2) the structure of the background currents, which promotes steepening of IT beams;

(3) considerable fluctuations of the thermocline and IT orbital currents are close in time, which indicates that stationary waves related to ITs coming from the straits are absent;

(4) large amplitudes of the barotropic current components perpendicular to the isobaths; and

(5) an insignificant "age" of the IT (the time between the greatest barotropic and internal tides).

It is especially difficult to establish the last sign since ITs radiate above a rapid arrive rather soon; therefore, the age of local ITs slightly differs from that of nonlocal waves.

The present work studies the peculiarities of IT wave generation near Oahu Island (Hawaii) based on an analysis of the hydrophysical measurements while taking into account the approaches mentioned above.

DATA DESCRIPTION

To study the characteristics of IT waves at the Oahu shelf, we used the results of the hydrophysical measurements performed in the Mamala Island water area in 2003–2004 [5, 11, 12, 14, 15, 18, 19]. In 2002–2004, the anthropogenic impacts of the sewage discharge from Honolulu into deep water on the coastal water area ecosystems were studied in this region of the Pacific in the scope of an international project [1, 5, 11, 12, 14, 15, 18, 19]. The hydrophysical characteristics

were measured using a number of moored buoys equipped with thermistor arrays and acoustic current meters (ADPs), onboard CTD and XBT sensors, and towed microstructure sensors (MSSs) [5, 11, 14, 19]. In addition, the survey was performed using different satellites [1, 2, 3, 11, 13, 15, 18].

Figure 1b shows the position of the moored buoys mounted at the shelf edge that were used to measure the vertical temperature profiles (points At, Bt, Ct, and Dt) and three current vector components (points Av, Bv, and Cv). The thermistor arrays and ADPs were located nearby [3, 11, 14].

The measurements were performed in three areas of Mamala Bay (see Fig. 1b): near the deep-water outfall diffuser (points At, Dt), at a distance of ~3–5 km east of the diffuser (points Bt, Bv), and at a distance of ~7 km southeast of the diffuser (points Ct, Cv). The currents were measured at depths of 4–76 m at spatial and time intervals of 2 m and 1 min, respectively. The water temperature was measured at different levels from 3–18 to 45–76 m at intervals of 2–5 min and 30 s in 2003 and 2004, respectively [5, 11, 14]. The accumulated data make it possible to study the variability of the hydrophysical characteristics in Mamala Bay on scales from several minutes to 20 days while taking into account the discreteness and duration of the measurements.

BACKGROUND CHARACTERISTICS IN MAMALA BAY

The conditions of IT wave generation depend on the topographic features, tidal currents, density stratification, and background currents in the region under study.

The Mamala Bay bathymetry is presented in Fig. 1d. The bottom inclination is ~0.1 near the coast and increases to 0.2–0.3 with increasing distance from the coast (Figs. 1e, 1f). The bottom areas that are very close to the coast are characterized by rugged topography. At depths of 10–75 m, the bottom is mainly flat but includes canyons and reefs [10].

The shelf depths are mainly about 50 m. The depth gradually increases to 600 m in the eastern bay and abruptly increases to 5000 m in the western area. The depths mainly increase southward and southwestward. The very narrow and steep shelf in Mamala Bay changes into a very steep slope at a distance of 2–3 km from the coast at depths of 70–80 m (see Fig. 1d).

The tidal currents in Mamala Bay rotate counterclockwise describing ellipses elongated along isobaths and are especially strong in the western bay [9, 17, 21, 23]. The density stratification of the water in Mamala Bay strongly varies not only in the seasons but also depending on the weather conditions and current variability [5, 10]. In 2003, the thermocline was closer to the bottom than in 2004, which was possibly related to the strong mixing of the upper layer during the Jimen typhoon that passed near Hawaii on September 2, 2003, and affected the current field [5]. The vertical density distributions in 2003 and 2004 are illustrated in Figs. 2a and 2b, respectively.

Figure 3 demonstrates the vertical distributions of the averaged current velocities at station A in 2003 and 2004 (panels 3a, 3b and 3c, 3d, respectively), which inform about the differences in the background currents in these years at different depths. A strong southwestward current jet (up to 0.5 m/s) was observed in the topmost oceanic layer in 2003, whereas the currents were much weaker, relaxed not so abruptly with increasing depth, and were mostly eastward–southeastward in 2004.

To estimate the background (i.e., not distorted by waves) buoyancy frequency, we developed a method that makes it possible to use the data of soundings performed during different tide phases. This is related to the fact that specific density profiles during different soundings can substantially differ from the background profiles due to the effect of strong internal waves.

The usually applied estimation of the background density stratification by averaging density profiles measured in the studied region is incorrect because the pycnocline obtained in this case is indistinct in depth, i.e., becomes less sharp and thicker than in the case when the stratification is undisturbed by waves. A buoyancy frequency profile estimated using such data does not characterize the background stratification and cannot be adequately used to theoretically calculate the internal wave parameters, especially when the pycnocline is sharp and the amplitude of its vertical variations is large. Therefore, the following approach was developed in order to eliminate such profile smearing:

(1) The set of density profiles $D(z)$ measured at different stations was formed.

(2) The density gradients $grad(D)$ were constructed for each density profile.

(3) The gradients were averaged $\langle grad \rangle (D)$ for each density value during all the soundings.

(4) The $grad(D)$ values averaged in such a way were used to calculate the buoyancy frequency background profile from a depth $\langle N \rangle (z)$. The average density profile $\langle D(z) \rangle$ is used to go from the density to depth.

The application of this technique to the calculation of the buoyancy frequency background value (based on the MSS density profile measurements in the vicinity of the diffuser in 2004) is illustrated in Figs. 4a and 4b. The dashes in Fig. 4b show the approximation proposed in [26] at the appropriate pycnocline parameters: the buoyancy frequency maximum is $Np = 15$ cycle h^{-1} at a depth of $Hp = 55$ m, and the pycnocline thickness is $dH = 70$ m. Figure 4b indicates that the buoyancy frequency background values are underestimated when the average density profile is used to determine N.

We also note that the buoyancy frequency background value is rather large (about 10 cycle h^{-1}) even above the beginning of a slope; therefore, the bottom inclinations near the shelf edge are supercritical under

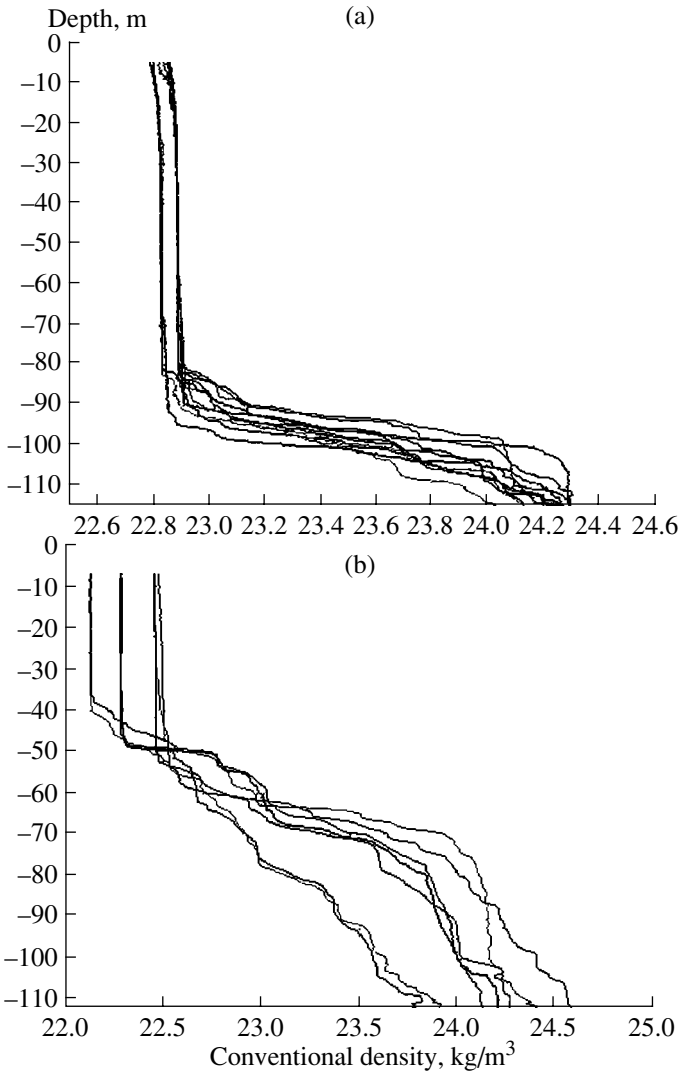

Fig. 2. Vertical profiles of the water density in Mamala Bay according to the measurements performed in (a) 2003 and (b) 2004.

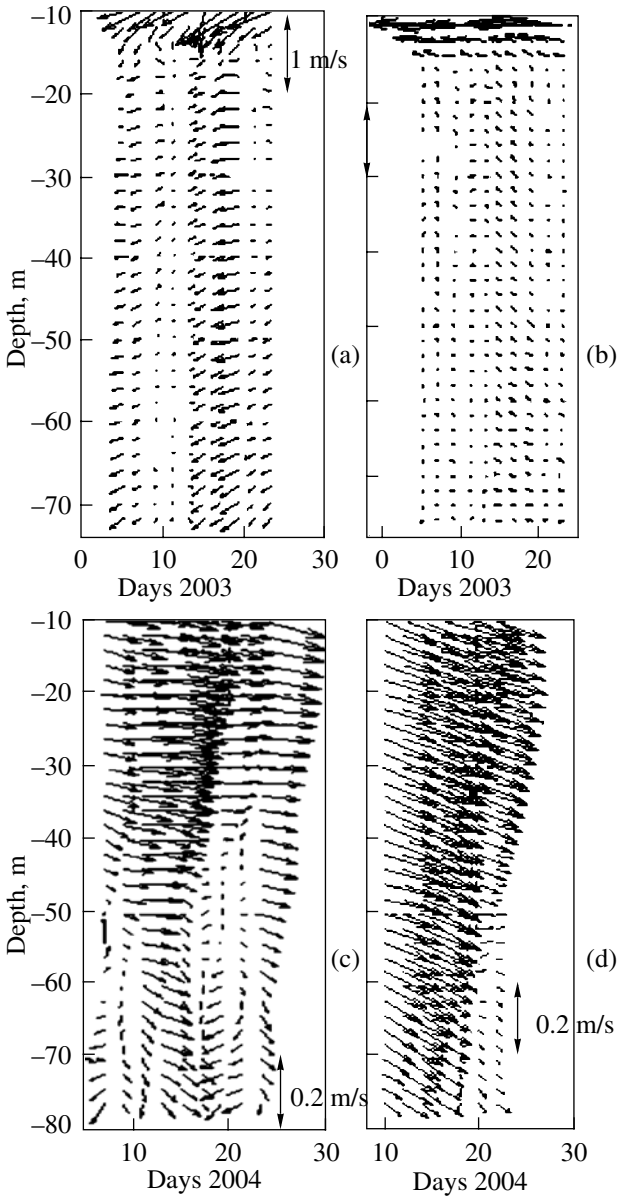

Fig. 3. Background (smoothed over two days) currents at points (a) Av, (b) Bv in 2003, (c) Bv, and (d) Cv in 2004.

average background conditions. For example, the IT beam inclination is 0.01 in the 200–300 m layer, where the buoyancy background frequency is close to 7 cycle h^{-1}, whereas the bottom inclination is an order of magnitude higher (see Fig. 1d).

We should note that the proposed method for estimating the background stratification includes distortions related to the horizontal inhomogeneity of the density field. These can be the causes of increased buoyancy in the upper layer, where the density changes at different stations and remains unchanged in depth in the mixed layer.

INTERNAL WAVE TIDE PARAMETERS

An analysis of the ADP measurements indicated that the surface tide currents above an inclined bottom are not barotropic (i.e., are variable over the vertical) and include the baroclinic component even in an unstratified ocean in contrast to such currents above a flat bottom. Therefore, it is incorrect to detect currents related to internal waves simply by subtracting the current averaged over the vertical, as is usually done.

It seems more reasonable to detect internal waves by expanding the tidal current field into orthogonal components (modes) by using the empirical orthogonal functions (EOFs), which have been widely used to analyze different physical processes [8, 22]. It is natural to assume that the lowest EOF mode belongs to the surface currents. In this case, the difference in the current fields between the observed field and the lowest (zero)

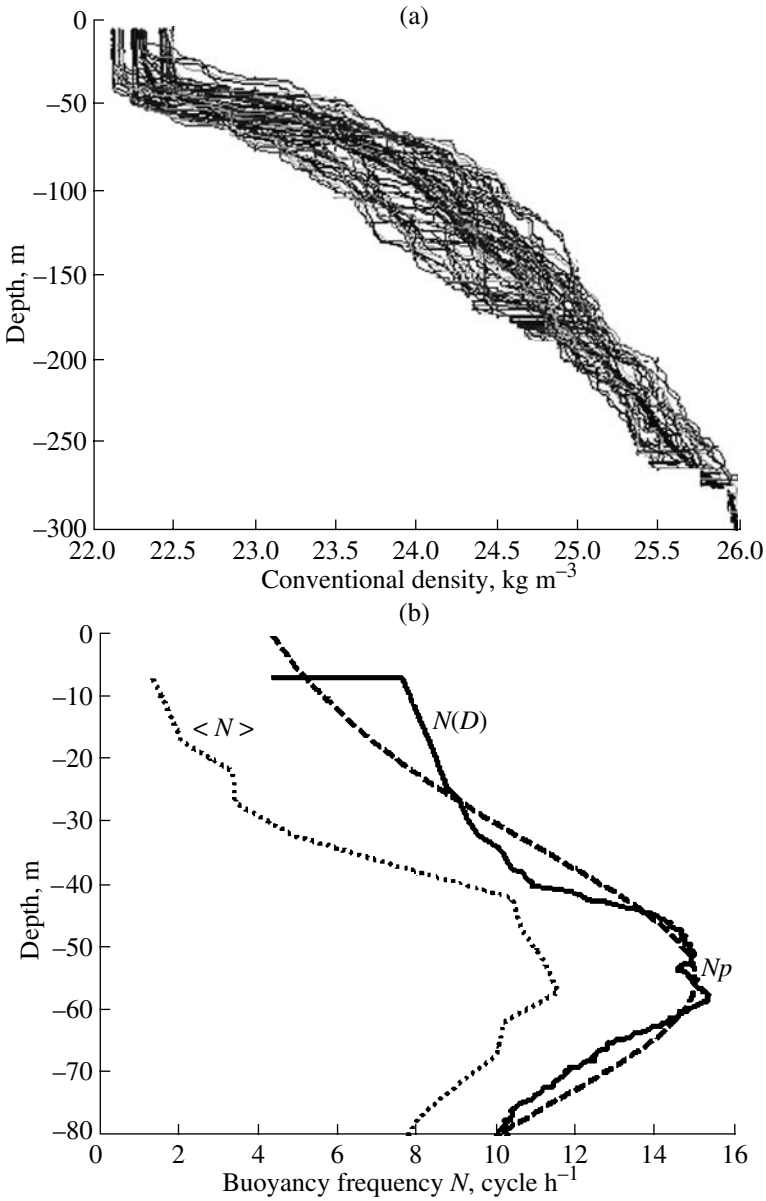

Fig. 4. Calculated background values of the buoyancy frequency: (a) the density profiles $D(z)$ at Mamala Bay according to the MSS measurements in 2004; (b) the background $N(D)$ and average N buoyancy frequency profiles and the $N(D)$ approximation from [26].

EOF mode can be considered to be the currents in internal waves, which are represented by the higher-order EOF modes.

A comparison of the EOF mode profiles (constructed based on the measurements of semidiurnal currents) and the dynamic mode profiles, which were constructed using the equation of internal waves for the existent stratification parameters, indicated that the mode profile shapes are in good agreement.

Based on the above procedure for detecting internal waves, we subtracted the sums of the EOF modes (0–1, 0–2, 0–3, etc.) from the observed field of currents. This made it possible to obtain the currents in the field of higher-mode internal waves (correspondingly, higher than modes 1, 2, 3 and so on).

We now analyze the internal wave fields in 2003 (calculated with the help of this technique) using the current measurements at point A as an example. These fields are presented in Fig. 5, which indicates that oblique fluctuations of the meridional (i.e., normal to the isobaths) current velocity are more pronounced in the field including high-order modes (Fig. 5d). This indicates that the corresponding waves are of local origin. Indeed, it is difficult to anticipate that high-order modes can penetrate in the studied region from distant sources, especially if we take into account the strong background current in the upper layer (Figs. 3a, 3b),

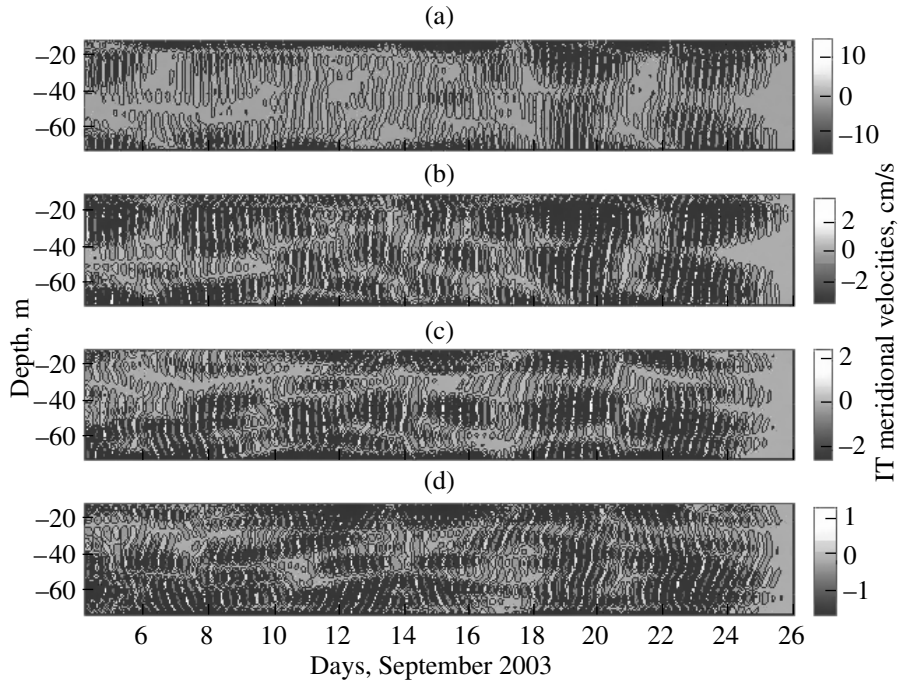

Fig. 5. (a) The field of the IT meridional velocity and ITs without (b) mode 1, (c) modes 1 and 2, and (d) modes 1–3.

which becomes critical even for IT mode 2. This is related to the fact that an internal wave is absorbed in the current with a vertical shift at the level where the current velocity becomes equal to the phase velocity of this wave [7].

Assuming that the field of the IT high-order modes is radiated near the site of the measurements, we detect the corresponding oblique wave, the form and energy of which propagate down and up, respectively. This part of the meridional current field, separated from the total spectrum of high-mode ITs (see [6]), is shown in Figs. 6a and 6b. It is much simpler to analyze the currents of the IT total field (Fig. 6a) and the field of high-mode upward waves (Fig. 6b) since these currents vary more smoothly.

A similar procedure was applied to all the other measurements of the currents, after which the pattern of the corresponding wave orbits was constructed (see Fig. 7). The orbits of the currents in the waves of local origin should correspond to Sverdrup flat internal waves, whose currents rotate clockwise and orbits are stretched along the normal to the isobaths with the ratio of the minor axis to the major one equal to $f/M2$ (0.38 in the studied region). We will call such orbits regular. The results of the processing indicated that more or less regular orbits of IT of local origin were reliably observed only at points A in 2003 and C in 2004, which are described by the thick lines in Figs. 7a and 7c, respectively. At point B in 2003 (Fig. 7b), such orbits existed only for a short time near the bottom and surface at the beginning and end of the records, respectively. At point B in 2004 (Fig. 7d), regular orbits were almost absent.

IT CHARACTERISTICS

First, we discuss the use of EOF for separating the surface and internal waves. Figure 8 presents the plots demonstrating a difference between the baroclinic tidal currents (without the current velocity values averaged over the vertical) and the currents in the ITs (after the subtraction of the lower EOF mode from the total tidal currents). The analysis of the plots presented in Figs. 8a–8c indicates that the difference between the baroclinic and IT currents (Fig. 8c) is rather considerable, especially at the top and bottom, which is related to distortions of the surface tide currents above the inclined bottom and to the effect of the strong current near the surface (see Figs. 3a, 3b).

The application of the method for detecting the waves of local origin made it possible to substantially simplify the IT field pattern by eliminating the low-mode components. The invariants of the field of baroclinic currents (without the values average over the depth) are characterized by a strong spatio-temporal variability—"orbit dancing"—due to the interference of different waves [4]. The field of only high-mode upward waves is much simpler, varies smoother (Fig. 6), and shows clearly defined zones of regular orbits, which can be considered to be a predominant manifestation of the waves of local origin.

The plots of the daily hodographs at isolated levels give a more evident, although less detailed, pattern of variations in the orbits of ascending high-mode IT waves (Fig. 7).

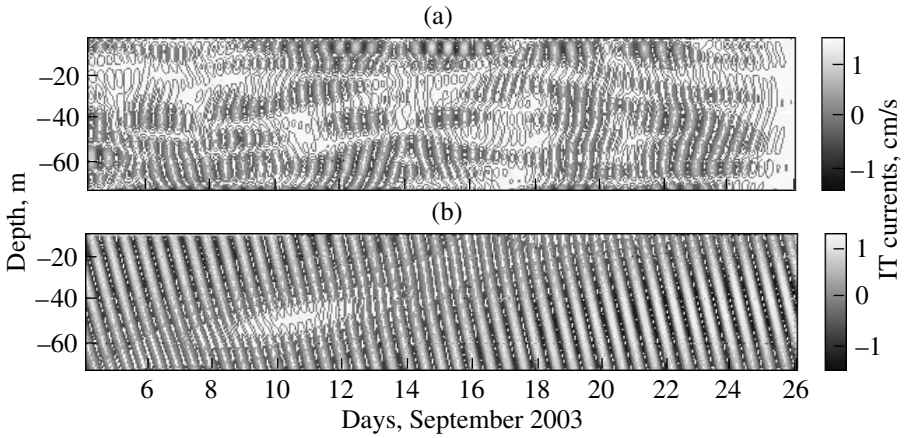

Fig. 6. The IT meridional currents without modes 1–3 at point A in 2003: (a) the IT total field and (b) the field of ascending currents.

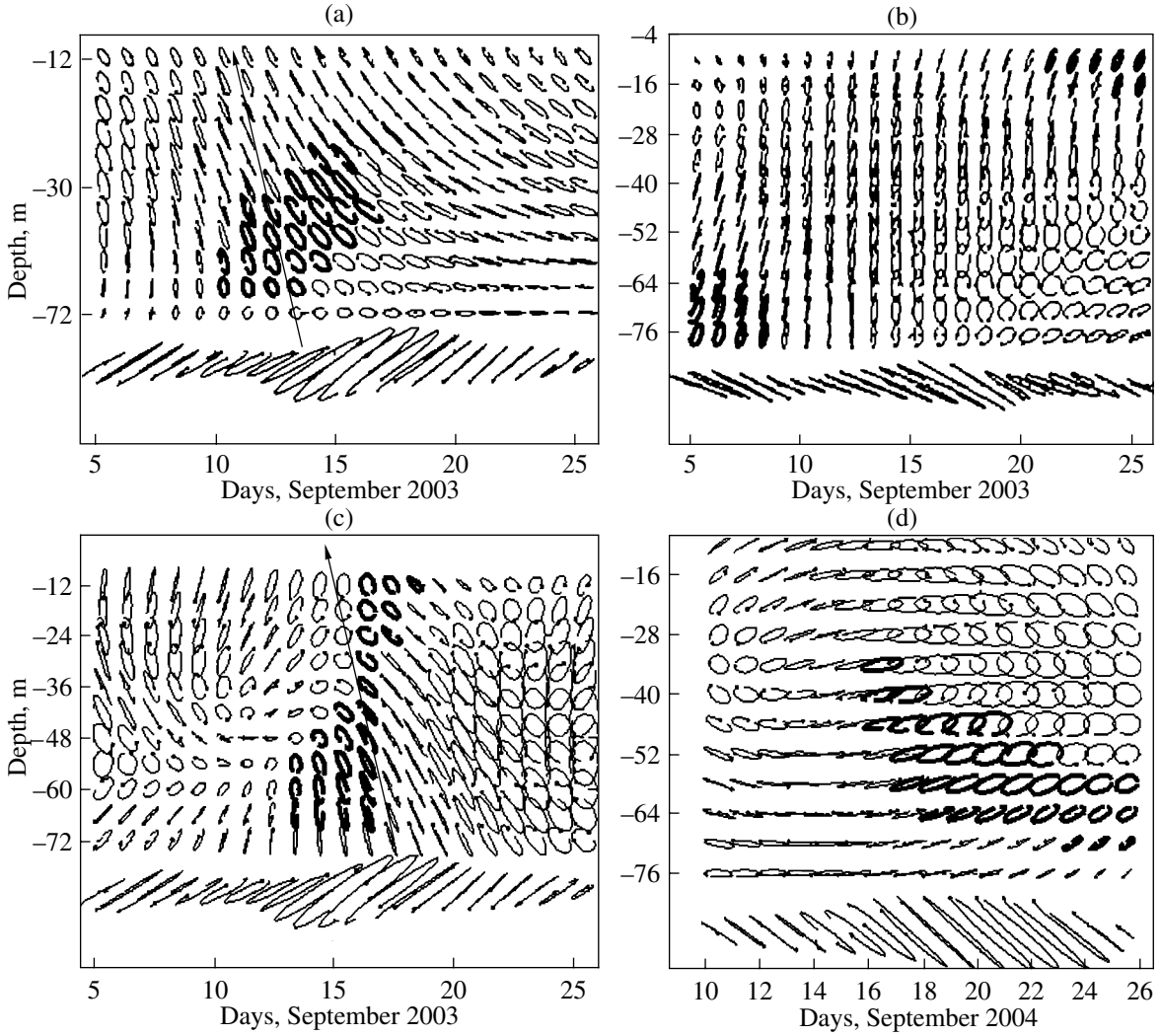

Fig. 7. Hodographs of the high-mode (higher than modes 3 and 4) IT currents calculated according to the measurements in Mamala Bay performed at (a) point A in 2003 (higher than mode 4), (b) point B in 2003, (c) point A in 2003 (higher than mode 3), and (d) point C in 2003. The hodographs for the EOF zero modes at the bottom are presented in the lower panel.

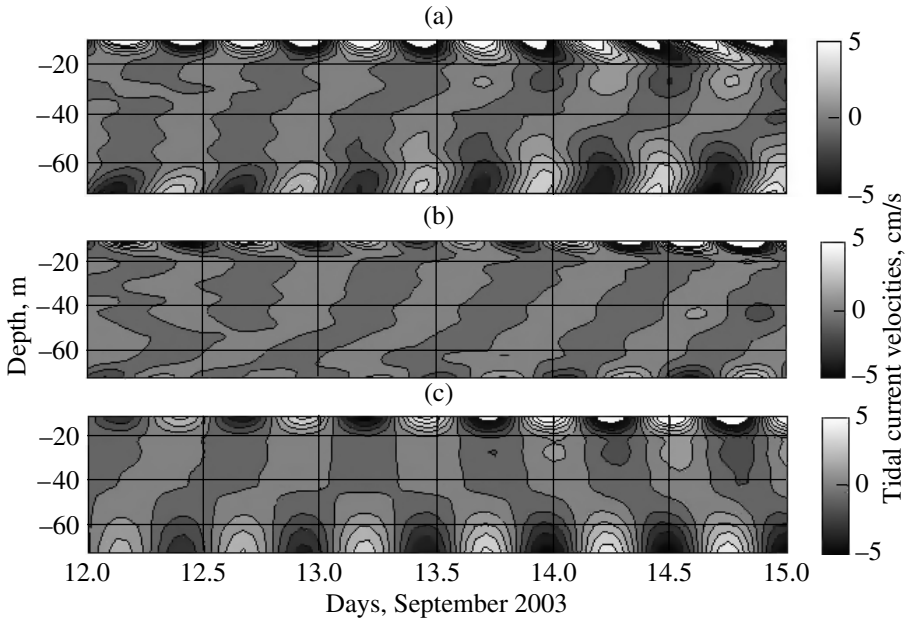

Fig. 8. Fragment of the tidal current record at point A in 2003: (a) baroclinic currents, (b) IT currents, and (c) the difference between these currents.

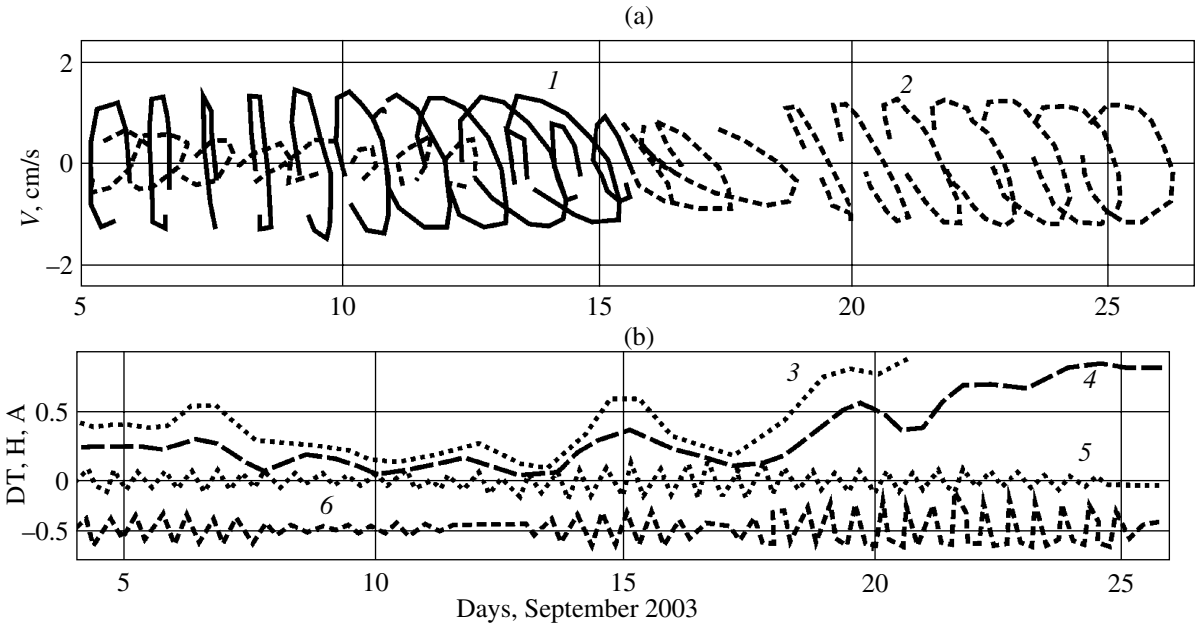

Fig. 9. Hodographs of the currents of ascending IT waves and the ambient parameters at points A and B in 2003: (a) the current hodographs at point A in 2003 at the level of 60 m without modes 0–3 (orbit *1*) and 0–4 (orbit *2*), (b) the smoothed (over 48 h) temperature difference (*DT*) between the upper and lower array sensors at points B (curve *3*) and A (curve *4*), the zero mode of the IT meridional currents at the bottom (in m/s, curve *5*), and the fluctuations of the 26.4° isotherm (in hundreds of meters, curve *6*).

It is natural to consider that the orbit "regularity" is the sign of locally studied Sverdrup elementary modes not distorted by other waves because the high-mode components of waves from distant sources weaken in the course of their propagation from their generation regions to the site of the measurements and under the action of the strong background current in the upper layer (Figs. 3a, 3b). Nevertheless, the "regular" pattern of orbits is sometimes masked by other waves because the remains of higher modes from distant sources and Kelvin internal waves [16], which are quite probable in this region, can be added to the waves of local origin.

The analysis of the orbit hodographs for high-order IT modes (higher than mode 3) shown in Fig. 7 for sta-

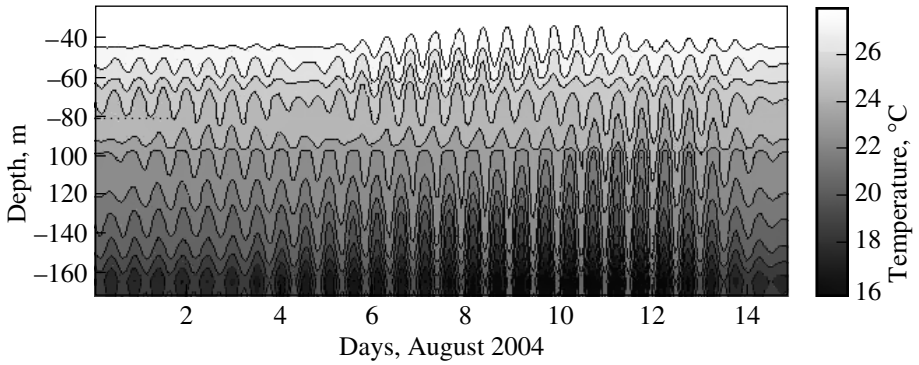

Fig. 10. Fragment of the semidiurnal fluctuations of isotherms at point D in 2004.

tions A–C in 2003 and 2004 indicates that local generation was most pronounced in the lower half of the water layer at point A in 2003 between days 11 and 17 of the observations, when the current orbits in the field of the ascending high-mode waves were more or less regular.

The hodographs of the IT orbits at point *av* in 2003 for the modes higher than 3 and 4 are presented in Figs. 7a–7c for comparison.

It is interesting that regular orbits also appear in the upper layer two–three days after their appearance in the bottom layer in the field of modes higher than 4 (Fig. 7b) in contrast to the higher-mode (higher than mode 3) field (Fig. 7a), which can be related to the upward motion of the group of waves radiating near the bottom. The estimated phase and group wave velocities confirm this assumption. When we estimate the phase velocity (Cz) based on the inclination of the meridional current contour lines (Fig. 5d, layer of 60–72 m, day 14), we find that $Cz = –0.84$ m/h, according to which $Cg/Cz \sim [1 – (f/\mathrm{M2})^2] = 1 – (0.38)^2 = 0.72$ m/h at the known ratio of the group (Cg) and phase velocities [6]. From this it follows that the waves will ascend from 60 to 10 m during 2.9 days, which coincides with the observations.

We also note that, near the bottom, regular orbits originate in the field of modes higher than 3 later than in the field of higher (higher than 4) modes (Figs. 7a–7c). However, the latter modes did not reach the upper layers, which can naturally be related to rapid damping of these modes.

In contrast to the high-mode waves observed at point A in 2003, neither the IT total field of this year nor the high-mode oblique waves at point B in 2003 and 2004 show so evident and stable signs of local generation. Indeed, at point B in 2003 (Fig. 7b), regular orbits of ascending waves existed for only a short time near the bottom (at the beginning of the records) and at the surface (at the end of the records); at the same time such orbits were altogether absent in 2004.

Taking into account the supercritical steepness of the bottom for the average stratification conditions in Mamala Bay, we can assume that the local generation will intensify at weakening of the bottom stratification since the IT beams become steeper in this case and the bottom inclination at the shelf edge approaches the critical value. Figures 1c and 1d, which present the bottom profile in the bay along three sections perpendicular to the isobaths, indicate that the bottom inclinations at the shelf edge were about 0.2.

Figures 9a and 9b present the hodographs of the IT ascending wave currents and the ambient parameters at stations A and B in 2003, which make it possible to reveal the most favorable conditions for the local generation of internal waves in Mamala Bay. Figure 9b presents the time variations in the temperature difference (DT) at the depths of the upper and lower sensors of the thermistor array at stations A and B, the depths of the 26.4°C isotherm, and the amplitude of the zero mode of the meridional currents at the bottom. The Density stratification at point A in 2003 weakened between day 8 and 14 of the measurements, when regular orbits of ascending IT high-mode waves were observed (Fig. 9a). In this case, regular orbits were observed in spite of the fact that the surface tide currents normal to the isobaths (zero mode bottom currents), which cause IT, were weak at that time (Fig. 9b, curve *5*). However, the fluctuations of the isotherms were also insignificant at that time (Fig. 9b, curve *6*), which testifies to the weakening of the IT total field where the waves from distant sources dominate. It is possible that the weakening of the waves from distant sources also favored the manifestation of waves of local origin.

A similar analysis of the ambient parameters and IT current characteristics was performed for station C in 2004, where the density stratification weakened insignificantly. Nevertheless, more or less regular orbits of ascending high-mode waves appeared in the second half of the period of measurements in the 50–70 m layer. Such a manifestation of local generation in the absence of weakened stratification can be an indication of the background current field being favorable for this generation, which can substantially affect the inclination of internal wave beams [20]. Even bottom areas, whose inclination in the absence of currents differs from the inclination of the beams, can become critical

under the action of the background current. Unfortunately, we have no information about the spatial structure of the background currents and cannot estimate the corresponding effects.

However, it is necessary to take into account that the sporadic appearance and occasional absence of regular orbits are apparently related not only and not so closely to the origination of conditions suitable for local generation as to episodic weakening of higher modes that propagate from distant sources and penetrate into the bay. It is natural to consider that IT waves are always radiated from the bay shelf edge but are usually masked by other stronger waves (including Kelvin ones [16]) and are sometimes observed in the pure form only in the field of high-order modes.

More intense local generation can be observed near the diffuser, where the bottom density stratification weakens under the action of the discharged fresh water. In this respect it is indicative that the semidiurnal fluctuations of the isotherms (according to the data of the thermistor array established slightly below the shelf edge at point D) demonstrate that the IT wave moves upward (Fig. 10). This motion corresponds to the downward propagation of the energy of the oblique wave apparently radiated from the outfall diffuser, which is located slightly higher than the thermistor array at the shelf edge.

CONCLUSIONS

Based on the performed analysis of the peculiarities of the semidiurnal ITs in Mamala Bay near Oahu Island, we can draw the following main conclusions:

(1) Internal tides, which are generated by distant sources and come from the straits bordering Oahu Island, predominate in the bay.

(2) Waves of local origin radiated from the shelf edge into the ocean are also present in the total field of the bay ITs.

(3) Local ITs are observed against the background of dominating waves of distant origin only in the field of short (high-mode) waves because the short-wave components of ITs from distant sources substantially weaken on their way to the bay and are replaced by local high-order modes.

(4) The circumstances favoring the intensification of IT generation and/or weakening of waves that come from distant sources promotes the appearance of locally radiated waves.

(5) The bottom inclinations at the bay shelf edge are supercritical for ITs everywhere except the area near the diffuser, where the buoyancy frequency can apparently decrease to critical values due to weakening of the bottom stratification.

(6) The critical and subcritical bottom inclinations at the shelf edge near the diffuser are responsible for the intensification of local generation and for the corresponding enhancement of an IT beam, which propagates from the diffuser upward into the open ocean and is reflected from its surface at a certain distance.

REFERENCES

1. V. G. Bondur, "Aerospace Methods in Present-Day Oceanology," in *New Ideas in Oceanology* (Nauka, Moscow, 2004), Vol. 1 [in Russian].
2. V. G. Bondur, Yu. V. Grebenyuk, and E. G. Morozov, "Registration from the Space and Modeling of Short Internal Waves in Coastal Zones of the Ocean," Dokl. Akad. Nauk **418** (4), 543–548 (2008).
3. V. G. Bondur and A. Sh. Zamshina, "Studying HF Internal Waves at the Shelf Boundary Based on the Spectra of Space Optical Images," Geodez. Aerofotos., No. 1, 85–96 (2008).
4. V. G. Bondur, K. D. Sabinin, and Yu. V. Grebenyuk, "Variability of Internal Tides at the Oahu Shelf (Hawaii)," Okeanologiya **48** (4), 1–11 (2008).
5. V. G. Bondur, N. N. Filatov, Yu. V. Grebenyuk, et al., "Studying Hydrophysical Processes during Monitoring of Anthropogenic Impacts on the Coastal Water Area (Using Mamala Bay, Oahu Island, Hawaii, as an Example)," Okeanologiya **47** (6), 827–846 (2007).
6. K. V. Konyaev, "Semidiurnal Inclined Internal Waves in the Pycnocline according to the Data on Vertical Current Profiles in the Arctic Regions," Izv. Ross. Akad. Nauk, Fiz. Atmos. Okeana **38** (6), 848–858 (2002).
7. K. V. Konyaev and K. D. Sabinin, *Waves within the Ocean* (Gidrometeoizdat, St. Petersburg, 1992) [in Russian].
8. M. I. Fortus, "Method of Empirical Orthogonal Functions and Its Application to Meteorology," Meteorol. Gidrol., No. 4, 113–119 (1980).
9. M. H. Alford, M. C. Gregg, and M. A. Merrifield, "Structure, Propagation and Mixing of Energetic Baroclinic Tides in Mamala Bay," J. Phys. Oceanogr. **36** (6), 997–1018 (2006).
10. *Atlas Hawaii*, 3rd ed. (Univ. Hawaii Press, Honolulu, 1998).
11. V. G. Bondur, "Complex Satellite Monitoring of Coastal Water Areas," in *Proceedings of the 31th International Symposium on Remote Sensing of Environment, St. Petersburg, 2005*, pp. 1–6.
12. V. G. Bondur and N. N. Filatov, "Study of Physical Processes in Coastal Zone for Detecting Anthropogenic Impact by Means of Remote Sensing," in *Proceedings of the 7th Workshop on Physical Processes in Natural Waters, Petrozavodsk, 2003*, pp. 98–103.
13. V. Bondur and S. Starchenkov, "Monitoring of Anthropogenic Influence on Water Areas of Hawaiian Islands Using RADARSAT and ENVISAT Radar Imagery," in *Proceedings of the 31th International Symposium on Remote Sensing of Environment, 2006*, pp. 184–187.
14. V. Bondur and M. Tsidilina, "Features of Formation of Remote Sensing and Sea Truth Databases for the Monitoring of Anthropogenic Impact on Ecosystems of Coastal Water Areas," *Proceedings of the 31th International Symposium on Remote Sensing of Environment, 2006*, pp. 192–195.
15. C. Gibson, V. Bondur, R. Keeler, and P. T. Leung, "Remote Sensing of Submerged Oceanic Turbulence

and Fossil Turbulence," Int. J. Dyn. Fluids (IJDF) **2** (2), 111–135 (2006).

16. P. Hamilton, "Observations of Tidal Circulation in Mamala Bay, Hawaii," in *Proceedings of the North American Water and Environment Congress, 1996.*
17. P. E. Holloway and M. A. Merrifield, "On the Spring-Neap Variability and Age of the Internal Tide at the Hawaiian Ridge," J. Geophys. Res. **108C**, JC001486 (2003).
18. R. Keeler, V. Bondur, and C. Gibson, "Optical Satellite Imagery Detection of Internal Wave Effects from a Submerged Turbulent Outfall in the Stratified Ocean," Geophys. Res. Lett. **32**, L12610 (2005).
19. R. Keeler, V. Bondur, and D. Vithanage, "Sea Truth Measurements for Remote Sensing of Littoral Water," J. Sea Technology, No. 4, 53–58 (2004).
20. E. Kunze, "Near-Inertial Wave Propagation in Geostrophic Shear," J. Phys. Oceanogr., No. 15, 544–565 (1985).
21. M. A. Merrifield and M. H. Alford, "Structure and Variability of Semidiurnal Internal Tides in Mamala Bay, Hawaii," J. Geophys. Res. **109**, C05010 (2004).
22. M. A. Merrifield and R. T. Guza, "Detecting Propagating Signals with Complex Empirical Orthogonal Functions: A Cautionary Note," J. Phys. Oceanogr. **20** (10), 1628–1633 (1990).
23. M. A. Merrifield and P. E. Holloway, "Model Estimates of M2 Internal Tide Energetics at the Hawaiian Ridge," J. Geophys. Res. **107C**, 3179 (2002).
24. M. A. Merrifield, P. E. Holloway, and M. S. Johnston, "The Generation of Internal Tides at the Hawaiian Ridge," Geophys. Res. Lett. **28** (4), 559–562 (2001).
25. A. A. Petrenko, B. H. Jones, T. D. Dickey, and P. Hamilton, "Internal Tide Effects on a Sewage Plume at Sand Island, Hawaii," Cont. Shelf Res. **20** (1), 1–13 (2000).
26. V. Vlasenko, N. Stashchuk, and K. Huttler, *Baroclinic Tides: Theoretical Modelling and Observational Evidence* (Cambr. Univ. Press, Cambridge, 2005).